MEASUREMENT OF SUBSURFACE FATIGUE CRACK SIZE USING NONLINEAR ADAPTIVE LEARNING

A. N. Mucciardi
Adaptronics, Inc.
McLean, Virginia 22101

I would like to present some ideas regarding the current status of fatigue crack NDE, where the field could go, and then give a case example of a recently synthesized NDE (software) system for detection and sizing aluminum fatigue cracks.

Currently, NDE training protocol requires calibrated test specimens. The specimens may not be appropriate, for example, for calibrating a crack detection system, and this creates problems. Detection is accomplished via amplitude thresholds and the amplitude, of course, is often ambiguous. Defect location is usually performed by the time-of-arrival factors. Multi-paths and other spurious reflections can give create "ghosts" which permit false readings to the place. Reliance on an operator to minimize problems such as low signal-to-noise also causes variability in detection probabilities. Additionally, operator difficulties in coping with complex geometries is troublesome. So, what I am proposing consists of another NDE protocol in which test specimens are used, but they are chosen to be much more appropriate for the task. Rather than simple flat bottom holes, one may have the type that Bernie Tittmann described previously, or others more germane to the problem. This will increase the cost of fabrication and also necessitate the training of a "smart" signal processor and interpretive system.

Instead of only examining the reflected echo amplitude, the entire signal must be examined in order to exploit properly the maximum information available. This is one of the reasons why increased reliance will be placed on a germane set of specimens.

Defect location can be estimated much more accurately by using special (phase) processing techniques to mask out ghosts and other spurious reflectors. The reliance on an operator can be minimized by enhancing the kind of display the operator sees and also by providing the person with more quantitative information. In terms of comparing the two, it is our estimate that the cost to upgrade current NDE equipment, (after its development) is between 5 and 10 K; the main addition is an in-line processor that we call a "smart instrument."

The cost of the test specimens required to make the processor "smart" depends upon the application. The benefits derived are improved, enhanced echoes for signal processing, less reliance on operator interpretation, improved time-of-arrival discrimination, and better ability to separate superimposed echoes. We can eliminate the reliance on amplitude thresholds and consequently, use all other characteristics of the signal except amplitude for improved size and orientation estimates.

This proposed practice has been developed and tested in off-line software, and the software exists for creating such a smart instrument. What we need is experience in determining what a representative specimen set is, some experience with on-line hardware, and the best structural form for this processor.

I would now like to present a case example of the proposed NDE practice in terms of a project that was sponsored by the Air Force Materials Lab regarding detection of subsurface fastener hole fatigue cracks in aluminum.

The test specimens were half-inch aluminum plates, 2 3/4 inches by 5 inches long, into which a one-fourth inch "fastener hole" was drilled. A notch was made on the lower surface - this was put in a fatigue bending jig, and a crack was grown out of the bottom of the hole. Two samples had no crack at all, and 14 other samples grew cracks ranging from 11 to 279 mils (see Fig. 1).

Specimen No.	EDM Starter Notch Depth*	Width**	Crack Length
00-000	---	---	0
01-000	---	---	0
02-011	.0026	.0022	.011
3-014	.0016	.0020	.014
4-018	.0016	.0019	.018
5-022	.0035	.0020	.022
6-027	.0020	.0020	.027
7-039	.0014	.0018	.039
8-048	.0019	.0020	.048
9-054	.0016	.0018	.054
10-073	.0019	.0021	.073
11-093	.0020	.0021	.093
12-113	.0024	.0019	.113
13-150	.0015	.0019	.150
14-192	.0017	.0018	.192
15-279	---	---	.279

*Depth along hole radius
**Width tangent to hole circumference

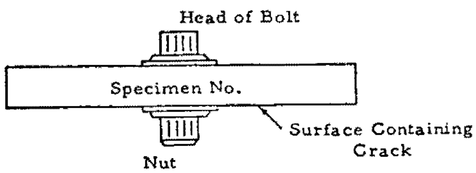

Figure 1. Crack lengths of specimens.

We wanted to not only detect cracks, but also to measure the subsurface crack length, particularly below 30 mils where detection presently is virtually nonexistent. The crack size range was logarithmically spread between 0 and 279 mils such that fifty percent of our sample cracks were less than 30 mils.

After the cracks had been grown, four more specimen cracks were grown in this range and destructively tested to verify the fact that we were dealing with quarter round cracks; that is, the surface length and the bore length were approximately equal. After the cracks were grown, a fastener was installed and torqued to the appropriate amount. Figure 2 schematically depicts the specimen plate without the fastener installed. The fastener hole and the crack are growing along the bottom surface. The crack is essentially a quarter round; the bore length and the surface length are nearly equal.

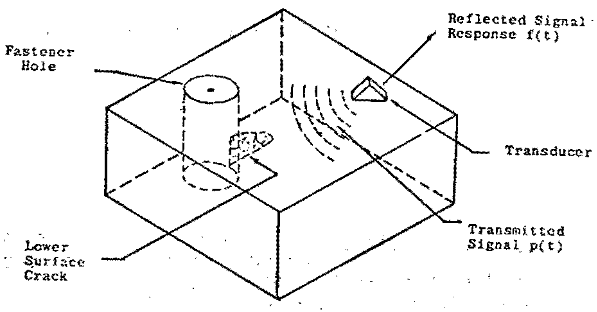

Figure 2. Simplified view of the ultrasonic test procedure.

The 10 MHz transducer is placed on a lucite wedge on top of the surface and an ultrasonic pulse is directed toward the crack at a 60° angle. The wave front interacts with a corner reflector made up of the hole, the bottom surface, and the crack. A reflection is transmitted back and recorded by the (same) transducer. The data were recorded by Bill Lawrie of Babcock & Wilcox.

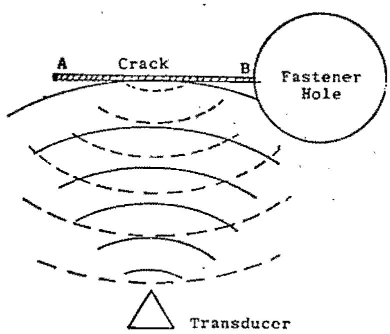

Figure 3. Illustration of interference effects as function of transducer viewing angle.
(a) wave patterns with transducer at normal incident position

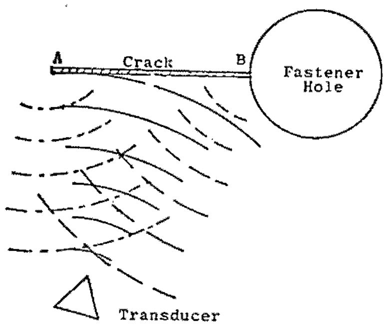

Figure 3. (b) Wave patterns with transducer at off-normal position

Figure 4 illustrates the kind of signal resulting from a corner reflector below the surface. This is an example of the base line noise level. There are really three events of interest.

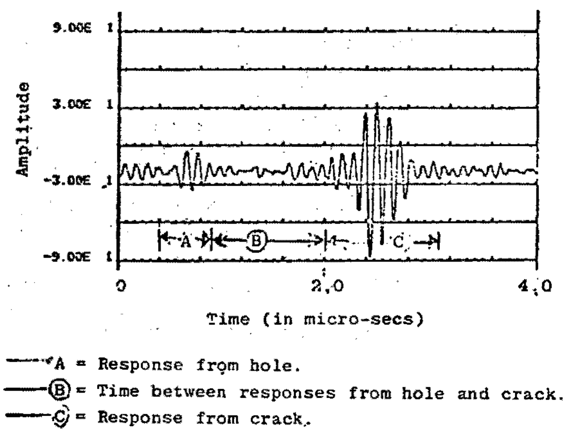

Figure 4. Response from 14-192 specimen viewed at $\theta = 0°$.

First of all, the beam comes in and hits the side of the hole. It continues to propagate until it encounters the crack. Echoes are recorded from the hole and crack reflections as shown in Fig. 4. The hole is always there; the crack may or may not be there. So, the objective is to first find the crack and then to determine its size.

Figure 5 illustrates some of the problems encountered if only amplitude is considered. These are actual echoes from just the portion of the signal due to the crack. Notice that the echo from the 93 mil crack is larger than the 192 mil crack.

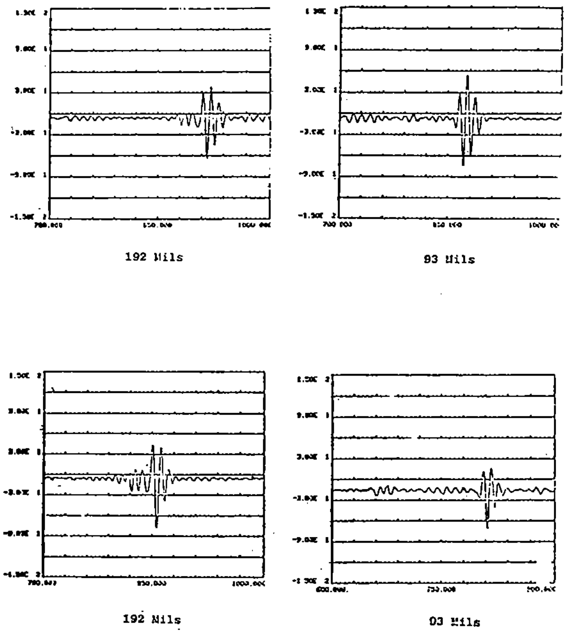

Figure 5. Ultrasonic waveforms recorded from two sample specimen cracks under different test conditions.

(a) Series 1: 192 and 93 mil crack signatures. Note the larger amplitude of the 93 mil crack. 1/

(b) Series 2: 192 and 93 mil signatures. 93 mil crack signature is considerably smaller.

1/The abscissa of each plot is time (μsec) and the ordinate is signal amplitude (arbitrary units).

It became evident that the fastener hole would have to be scanned in a circular manner to provide accurate estimates of crack size. Six viewing angles were chosen as shown in Fig. 6. The normal incident position is defined to be $\theta = 0°$. As θ increases, the incident beam is reflected from the hole and from the two edges of the crack (as shown in Fig. 3). As expected, large cracks (i.e., greater than 100 mils) are visible at all viewing angles Cracks between 50 and 100 mils in length are mainly visible only at $\theta = 0°$; while cracks below about 30 mils are very difficult to see, and in fact, nearly impossible to detect.

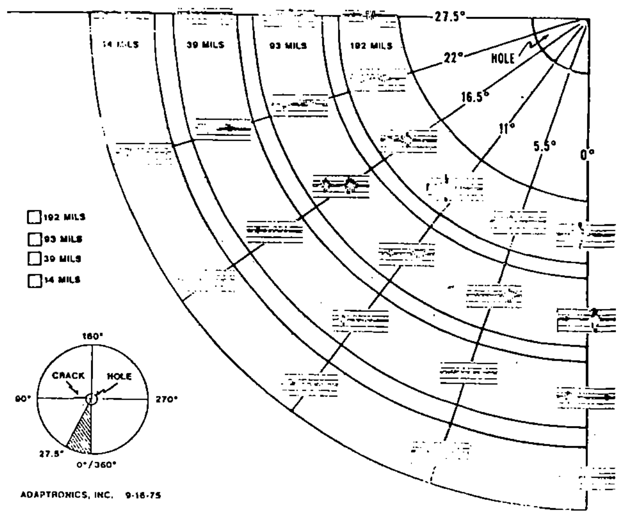

Figure 6. Ultrasonic scanning plan about hole.

We put together a (software) system to process this kind of information. Figure 7 is a scatter plot of our results showing the true vs. measured crack length, from zero to 279 mils.

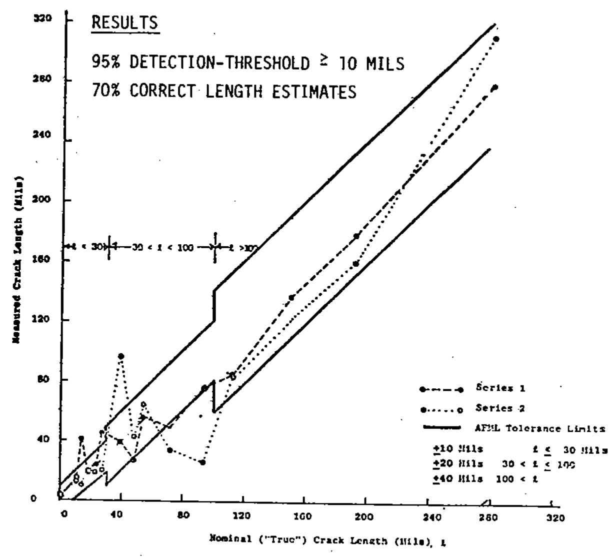

Figure 7. Performance of ALN quantitative surface/subsurface fatigue crack length measurement system

The tolerance limits on the curve are according to AFML: if a crack is truly larger than 100 mils, a 40 mil error would be tolerable; if it is between 30 and 100 mils, a 20 mil error would be tolerable; if it is below 30 mils, a 10 mil error would be tolerable. So, as you can see, the Adaptronics system has the ability to detect cracks across this range, and also has the ability to measure cracks within 70 percent of the true crack length--even down to 11 mils. In fact, the "no" crack specimens were classified as cracks of just a few mils length. Furthermore, if these results are recast in terms of probability of detection, a threshold can be placed at any position of the abscissa, parallel to the ordinate, and a count of those cracks that were truly larger than the threshold and which were correctly classified as larger than the threshold can be made. The percentage of correct calls is an estimate of the probability of detection for this threshold setting. This threshold can be varied between 10 and 200 mils, and it is found that correct detection of cracks occurs 95 percent of the time. Not only are 95 percent of the cracks detected, but in addition, our system can size cracks to within 70 percent of the true value, on the average. So, here is a quantitative NDE system that really works in an actual environment.

The details of how the system works can be summarized in the following way. The transducer beam is directed such that it first encounters the hole and then contacts the crack (when aligned in a normal incidence portion, the main portion of the reflected energy will be directed back to the transmitter). As the transducer is swung around the hole, the beam will be reflected from the crack edges; however, most of the energy will be reflected away from the transducer. The reflection will come from the two edges of the hole, A and B, as shown in Fig. 3 and, depending upon the frequency transmitted and the length of the crack, these waves that are returning from A will return sooner than B. The A and B echoes may or may not be in phase. If they're not, they will destructively interfere; if they are, they will constructively interfere. So, these interference patterns are functions of, among other things, the size of the crack.

One can use these interference patterns as a method of inferring the size of the crack. To do this, we built a jig to mount our transducer for data recording purposes. On that jig we made a little slit and attached the transducer. The transducer was clamped down at a fixed radius from the hole so we could swing the jig around, such that the transducer was always at a fixed distance from the center of the hole (see Fig. 8).

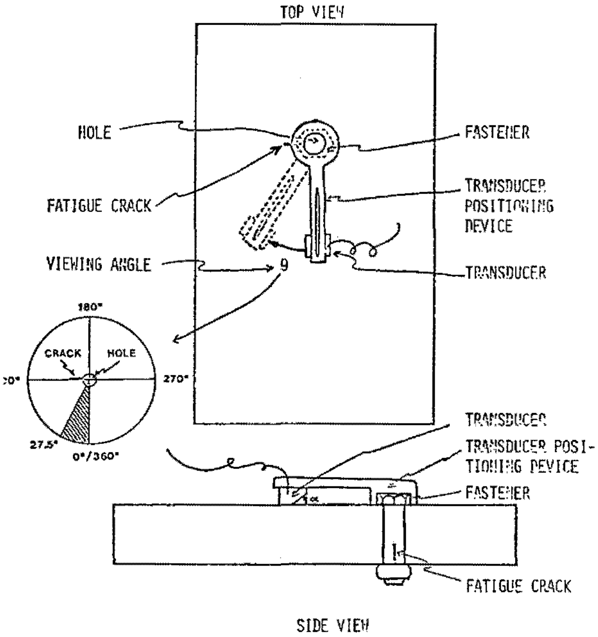

Figure 8. Fatigue crack ultrasonic recording equipment.

After a preliminary look at the data, we decided to record echoes between the normal incident position (which we defined to be $\theta = 0°$) up to 27.5 degrees away ($\theta = 27.5°$); we took 5.5 degree increments ($\Delta\theta = 5.5°$) which gave us six pulse echoes.

Signals were averaged to increase the signal-to-noise ratio. We determined that an average of 32 signals the optimum value because of the quantification level of our digital transient recorder (we were using an 8-bit, 2048-word biomation 8100 to digitize these transients). Digitizing at a rate of 50 MHz with an 8-bit transient recorder enabled us to accurately capture the 10 MHz transducer pulse echo. We determined that our usable frequency range was about plus or minus 4 MHz on either side of 10 MHz; or, 6 to 14 MHz.

The signal that is actually recorded is a composite of a number of subsytems: the pulser, the transducer that connects electrical energy to sound energy, medium, and finally, the discontinuity. Therefore, the recorded signal is sensitive not only to the defect but also to the transducer and the medium through which it propagates.

We wanted to minimize the effect of transducer and medium. To do this, the transducer was swung around to the side of the hole which had no crack. Another signal was recorded with the same transducer and medium but without the defect. Then, we deconvolved our "crack signal" with what we call our "reference signal." This was done by dividing by the reference signal in the frequency domain. Since the deconvolution process is a noise-inducing step, we had to filter the quotient signal to finally end up with a signal which was stripped somewhat of transducer and medium effects.

We then generated a number of parameters from these wave forms. Figure 9 is a plot of one of the parameters--total power--versus crack length the trend can hardly be called monotonic. This parameter was maximally correlated with crack size. This shows that no single parameter in a real environment is every going to be clearly correlated with crack size. However, even though there is no monotonic relationship with defect size, there is a general trend of increasing power with increasing defect size.

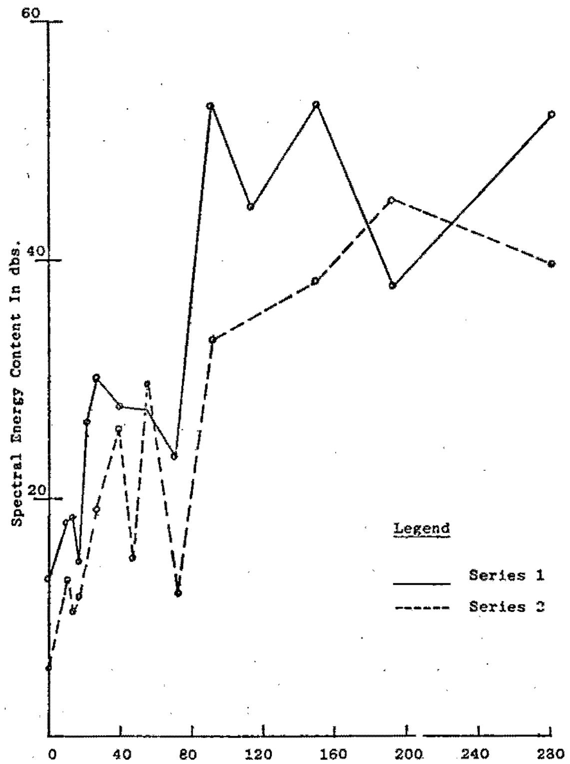

Figure 9. Plot of deconvolved total spectral energy versus crack length.

We generated a number of parameters from the power spectrum by dividing it into 1 MHz bands, and computing the percentage power in each band between 6 and 14 MHz. Small cracks ought to have more high frequency energy, whereas larger cracks should be more broad band. Other transformations were performed to look for echoes contained within the signal. A set of 31 descriptors or each echo were generated. A nonlinear polyramid model--called an Adaptive Learning Network--was synthesized. This ALN function mapped echo descriptors into a predicted defect size. The parameters are given in Table 1.

TABLE I. ALN Input Parameters

WAVEFORM	NUMBER	DESCRIPTION
POWER SPECTRUM	9	FRACTIONAL POWER IN 1 MHz BANDS IN RANGE 6 TO 14 MHz; TOTAL POWER
SPATIAL POWER	1	TOTAL POWER DIVIDED BY WIDTH OF SPATIAL RANGE
CEPSTRUM	20	NUMBER OF T's OBSERVED IN 10 EQUALLY SPACED BANDS BETWEEN 0 - 2, 700 NANOSECONDS; TOTAL CEPSTRAL VALUES IN THE 10 BANDS
TRANSDUCER ORIENTATION	1	SIN 9

TOTAL: 31

Since we wanted to be proportionately more accurate for below 30 mils, we modeled the logorithm of the crack length rather than the crack length itself. This spread the small values intende to bring in the larger values of crack size. What happens is that in synthesizing our model we forced it to be very sensitive to small errors in crack lengths below 30 mils and less sensitive about crack lengths above 30 mils (see Fig. 10.).

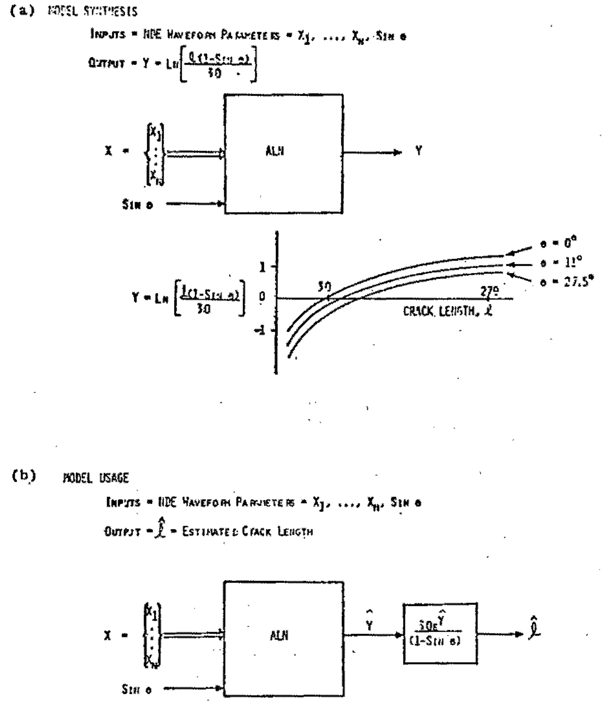

Figure 10. Quantitative surface/subsurface fatigue crack length measurement system.

You can also recast these results into a probability-of-correct acceptance curve. In current practice, very little detection capability exists below about 40 or 50 mils, so our system is very accurate indeed.

In terms of placing this NDE system into the field, a "teething ring" transducer array would be best for rapid inspection of fastener holes. The transducers would be electronically fired and computer processing such as that described above would be used to establish the most nearly normal incident beam as well as the remainder of the parameter generation and crack size estimation steps.

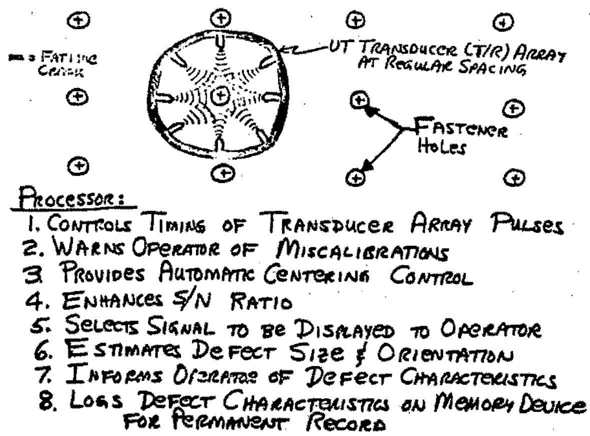

Figure 11. Schematic for "Teething ring" transducer array.

In the usage phase we record an echo, generate the necessary parameters, make an estimate of the crack size logarithm, and take the antilog to produce the length estimate. The results were tested on new data as well as some of the data that were used to synthesize the ALN model (see Fig. 7.).

In summary, we have demonstrated the first quantitative system (at least in this kind of environment) that can detect and measure cracks in this size range. It is also the first quantitative system to show high insensitivity to different transducers and materials. We can process a pulse echo all the way to a crack size estimate within a few milliseconds in software per fastener hole.

DISCUSSION

DR. PAPADAKIS: Thank you. This looks as if we are getting new solution packages which are beyond the things we have been taught to expect in the past.

Since we're running behind, I'm going to ask you to question privately.